International Journal of Pharmaceutics 391 (2010) 313–321

Contents lists available at ScienceDirect

International Journal of Pharmaceutics

journal homepage: www.elsevier.com/locate/ijpharm

Pharmaceutical Nanotechnology

Nanostructured lipid carriers constituted from high-density lipoprotein components for delivery of a lipophilic cardiovascular drug

Wen-Li Zhang[a], Xiao Gu[a], Hui Bai[b], Ru-Hui Yang[c], Chen-Dong Dong[a], Jian-Ping Liu[a,*]

[a] Department of Pharmaceutics, China Pharmaceutical University, 24 Tong Jia Xiang, Nanjing 210009, PR China
[b] Atherosclerosis Research Centre, Nanjing Medical University, Nanjing 210029, PR China
[c] Department of Pharmacology, China Pharmaceutical University, Nanjing 210009, PR China

ARTICLE INFO

Article history:
Received 7 December 2009
Received in revised form 26 January 2010
Accepted 2 March 2010
Available online 7 March 2010

Keywords:
HDL
Nanostructured lipid carrier
Electrophoresis
Phagocytosis
Apolipoprotein A-I

ABSTRACT

To investigate the possibility of reconstituted protein-free high-density lipoprotein (HDL) being a carrier for delivering a lipophilic cardiovascular drug, Tanshinone IIA-loaded HDL-like nanostructured lipid carriers (TA-NLC) were prepared by a nanoprecipitation/solvent diffusion method. The physicochemical parameters of TA-NLC were characterized in terms of particle size, zeta potential, morphology, entrapment efficiency, differential scanning calorimetry (DSC) and stability. A novel two-step method has been employed to determine entrapment efficiency of TA-NLC. The binding properties of TA-NLC to apolipoproteins were investigated by *in vitro* incubation competition assay in the presence of native HDL and electrophoresis test. Phagocytosis and cytotoxicity was evaluated using mouse macrophage cell line RAW 264.7 with TA-NLC and incubated TA-NLC with native HDL (TA-NLC-apo). The results showed that TA-NLC had an average diameter of 8.0 ± 1.2 nm, zeta potential of -29.0 ± 0.0 mV, drug loading of $6.17 \pm 0.3\%$ and entrapment efficiency of $97.84 \pm 1.2\%$. TA-NLC were demonstrated spheres with drug incorporated in lipid core forming a shell-core structure. DSC analysis showed that TA was dispersed in NLC in an amorphous state. The incorporation of glycerol trioleate to NLC led to crystal order disturbance. Agarose gel electrophoresis and sodium dodecyl sulfate polyacrylamide gel electrophoresis (SDS-SPAGE) patterns indicated that TA-NLC could bind to apolipoprotein A-I (apoA-I) specifically *in vitro*. Phagocytosis studies showed significant differences in uptake between TA-NLC and TA-NLC-apo and demonstrated that TA-NLC incubated with native HDL could turn endogenous by association to apolipoproteins, which cannot trigger immunological responses and could escape from recognition by macrophages.

1. Introduction

Tanshinone IIA (TA), one of the liposoluble active components extracted from the root of *Salvia miltiorrhiza Bunge*, is an effective cardiovascular agent which can dilate coronary arteries and increase myocardial contractility (Zhao et al., 1996). However, TA has a low bioavailability due to its negligible solubility in water, short half-life (Li et al., 2007b) and first pass metabolism (Hao et al., 2007). Recently, a number of strategies have been employed to address these issues, e.g., polymeric nanoparticles (Li et al., 2008), emulsions (Liang et al., 2008), microemulsions (Li et al., 2007a), proliposomes (Chu et al., 2002), nanoparticles (Liang et al., 2007) and so on.

In our previous studies, Tanshinone IIA-loaded solid lipid nanoparticles (TA-SLN) have been developed as a carrier system for its superiorities with manageable burst effect issue, prolonged circulation time, as well as increased AUC (Liu et al., 2005; Zhang et al., 2008). In recent years, nanostructured lipid carriers (NLC) as a new generation of lipid nanoparticles which consists of a mixture of spacially different lipid molecules, i.e., solid lipid is blended with liquid lipid, has been developed to overcome the disadvantages of solid lipid nanoparticles (SLN) such as limited drug loading, risk of gelation and drug leakage during storage caused by lipid polymorphism (Müller et al., 2002a,b). In view of this, NLC may be regarded as an alternative to SLN and appeared to be a novel approach for improving the delivery of TA.

Currently, Schöler et al. (2002) have reported that the nature of the lipid matrix and concentration of nanoparticles influenced their cytotoxic effects on macrophages. As known to all, a variety of different emulsifiers have been used for the preparation of SLN or NLC dispersions, including bile salts, poloxamers, and other ionic and nonionic surfactants which can induce irritative, hemolytic, or sensitizing action (Bunjes et al., 2003; Han et al., 2008; Joshi et al., 2008). Furthermore, animal experimentation and clinical studies have provided convincing evidence that metabolism of lipid was related to incidence of coronary heart disease (Kontush and Chapman, 2006). Therefore, lipid matrices and surfactant should

* Corresponding author. Tel.: +86 25 83271293; fax: +86 25 83271293.
E-mail address: liujianpingljp@hotmail.com (J.-P. Liu).

0378-5173/$ – see front matter © 2010 Elsevier B.V. All rights reserved.
doi:10.1016/j.ijpharm.2010.03.011

be even more carefully chosen and tested for later intravenous use when a cardiovascular agent is encapsulated in lipid nanoparticles. Thus, by using proper matrices for NLC, i.e., preparing NLC from endogenous substance in blood without surfactant, it is possible to solve issues of conventional NLC related to intravenous use.

High-density lipoprotein (HDL) is a heterogeneous class of plasma lipoproteins that have a density between 1.063 g/ml and 1.210 g/ml and a Stoke's diameter of 5–17 nm (Assmann and Nofer, 2003). HDL is composed of a hydrophobic core of triglycerides and cholesterol esters covered in a monolayer of phospholipids into which apolipoprotein A-I (apoA-I) is embedded (Thaxton et al., 2009; Libby et al., 2008; Silva et al., 2008; Ajees et al., 2006; Thomas et al., 2008). ApoA-I, which is comprised of 10 amphipathic alpha helices each with a hydrophobic domain and a negatively charged hydrophilic domain, is the main protein component of HDL and defines the structure and physiology of HDL *in vivo*. HDL is a dynamic serum protective against the development of atherosclerosis and resultant illnesses such as heart disease and stroke (Vance and Vance, 2002).

In the past decades, various research groups have been successful in development of recombinant HDL (rHDL), with physicochemical properties similar to those of native HDL. rHDL infusion has shown therapeutic promise for regression of atherosclerotic lesions (Linsel-Nitschke and Tall, 2005; Eriksson et al., 1999). Recently, rHDL has been utilized as a delivery vehicle for many lipophilic drugs (Lou et al., 2005; McConathya et al., 2008; Oda et al., 2006) due to its attractive attributes including favorable structure, target effect, endogenesis, a long circulation time in plasma with a $t_{1/2}$ of 3.8–6.2 days (Herbert et al., 1984) and capacity to escape from recognition and elimination by reticuloendothelial system (RES) (Rensen et al., 2001).

However, a limitation for the therapeutic application of rHDL is the necessity to isolate HDL apolipoproteins from human serum or resort to cell expression systems that secrete recombinant human apoA-I (Mallory et al., 1987; Pyle et al., 1996). In addition, the procedures to gain apoA-I are very sophisticated in order to avoid immunological responses aroused by heterology. Therefore, reconstituting an alternative HDL-like model, which is prepared from lipid portion without incorporating apolipoproteins, will be a promising outlet. In fact, Maranhao et al. (1993) has clearly established that apolipoprotein-free lipid emulsion resembling low density lipoprotein (LDL) behaved similarly to native LDL when injected into rats and human subjects (Maranhao et al., 1994). Hence, biomimetic HDL-like NLC may also be constituted from lipid portion of native HDL without apolipoproteins, which is more favorable to industrial production.

On the ground of related literatures, the following three prerequisites should be met to ensure NLC mimic the native HDL when drug was incorporated: (1) The size of TA-NLC should be small enough to display same fate with the native HDL *in vivo* (Frias et al., 2006); (2) Among the various components of HDL, apoA-I is believed to be the main apolipoprotein defining the structure and physiology of HDL (Calabresi et al., 2006), hence TA-NLC should bind to apoA-I after intravenous injection; (3) Lipophilic drugs incorporated into the lipid moiety of NLC should not interfere with the receptor-mediated recognition of apolipoproteins (Pyle et al., 1996; Cormode et al., 2008).

In this paper, the lipid matrices of conventional NLC were substituted by components of native HDL from the standpoint of engineering a naturally long-circulating and health beneficial nanoplatform as well as stable and high drug loading without using surfactant. The present study was to prepare protein-free HDL-like TA-NLC with properties such as size range, shape and composition resembling HDL, to explore the potential of TA-NLC binding to the main apolipoprotein in HDL by *in vitro* incubation and macrophage studies.

2. Materials and methods

2.1. Materials

Tanshinone IIA was purchased from Luoyang Pharmaceutical Co. Ltd. (China). Lipoid S 100 was obtained from Lipoid GmbH (Germany). Cholesterol was purchased from Sigma–Aldrich chemie GmbH. Cholesteryl oleate was supplied by Alfa Aescar/Johnson matthey Co., Ltd. Glycerol trioleate was product of Tokyo Kasei Kogyo Co., Ltd. (Japan). Human plasma was supplied from Nanjing Red Cross. RAW 264.7 cells were obtained from American Type Culture Collection. Potassium bromide (KBr) was purchased from Xi'an chemical reagent Co., Ltd. (China). All reagents used were of analytical grade except methanol of chromatographic grade.

2.2. Preparation of TA-NLC

Natural HDL consists of apolipoproteins, polar lipids (phospholipids and cholesterol), and nonpolar neutral lipids (predominantly cholesterol esters and triglycerides). The proportions of 4 components for TA-NLC are the same with those of natural HDL. Both phospholipids and cholesterol are commonly used as helper lipids in the liposomal formulations, which are known to improve the stability.

TA-NLC were prepared by a nanoprecipitation/solvent diffusion method (Fessi et al., 1989). Cholesteryl oleate and phospholipid were used as solid lipid material and glycerol trioleate was used as liquid lipid material. Typically, Tanshinone IIA, cholesteryl oleate (>97% pure, 29%, w/w), glycerol trioleate (>80% pure, 13%, w/w) and cholesterol (>95% pure, 6%, w/w) were dissolved in acetone (8 ml) by sonication (DL-720, Shanghai, China), then soybean lecithin (>97% pure, 46%, w/w) dissolved in 2 ml of absolute ethanol was added to acetone to form an organic phase maintained at $60 \pm 2\,^{\circ}C$. Then the organic phase was injected slowly into an aqueous phase of the same temperature, which contains 0.1 M KC1, 1 mM EDTA and 0.01 M Tris–HCl, pH 8.0 in double distilled water (30 ml). Then a semi-transparent pre-emulsion was obtained under constant magnetic agitation. After ultrasonication for 200 s using Ultrahomogenizer (JY 92II, Ningbo, China), the dispersion was transferred to a rotary evaporator to remove organic solvent at 65 °C under reduced pressure. The prepared TA-NLC were filtered through 0.22 μm filters after cooling down to room temperature, then stocked at 4 °C in the dark.

2.3. Preparation of TA-NLC-apo

2.3.1. Isolation of HDL

Native HDL was obtained from the blood of healthy normolipidemic donors by two-step ultracentrifugation.

The final density of 10 ml of plasma in a 11 ml ultracentrifuge tube (Polyallomer Bell-top; Beckman) was adjusted to 1.063 g/ml with solid KBr according to Radding–Steinberg formula (Radding and Steinberg, 1960):

$$X = \frac{V(d_f - d_i)}{1 - 0.312 \times d_f}$$

where X is grams of KBr, d_i is initial density, d_f is final density, V is volume of the serum in ml, and 0.312 is partial specific volume of KBr.

The ultracentrifuge tube was sealed using a Beckman Tube Topper Sealer. Ultracentrifugation was performed in a Beckman Optima LE-80K Table Top at $195{,}000 \times g$ (24 h) and 4 °C in a Beckman fixed-angle rotor (TL100.3). Upon completion of ultracentrifugation, the supernatant (VLDL and LDL) that float above the background solution with density below 1.063 g/ml was removed

by aspiration with a needle. The remaining solution (corresponds to HDL and plasma proteins existing at the bottom of tube), was adjusted to a background density of 1.210 g/ml by adding solid KBr. A second ultracentrifugation step was then performed with the same procedure mentioned above. Then the top layer of yellow liquid was collected by aspiration and dialyzed at 4 °C in the dark against 4 changes of 2 l of 0.15 M NaCl, 1 mM sodium EDTA, and 0.01 M Tris–HCl buffer overnight to remove KBr contained in the solution. The final concentration of native HDL obtained was 2 mg/ml.

2.3.2. In vitro incubation of TA-NLC with native HDL

TA-NLC (8 ml) were incubated with 2 ml of HDL for 4 h on a shaking bed (SHZ-82A, Jintan, China, 120 rpm, 37 °C). After incubation, the density of incubated mixture was adjusted to 1.063 g/ml with solid KBr. Then the mixture was submitted to ultracentrifugation at 195,000 × *g* at 4 °C for 24 h. After ultracentrifugation, excessive TA-NLC which floated above the background solution was removed by aspiration with a needle. Then the orange liquid layer appearing at the bottom of the tube was recovered and dialyzed against 4 changes of 2 l of 0.01 M Tris–HCl buffer, containing 0.15 M NaCl and 1 mM EDTA. This orange solution obtained was termed as TA-NLC-apo to show distinction from TA-NLC.

2.4. Determination of Tanshinone IIA in TA-NLC

The amount of Tanshinone IIA incorporated in TA-NLC was determined after dissolution in absolute ethanol. Blank NLC were determined to evaluate the interference of excipients. TA in drug-loaded NLC was determined by HPLC (Shimadzu LC-10A, Kyoto, Japan) equipped with an ultraviolet (UV) detection operated at 268 nm and a Shim-pack VP-ODS (150 mm × 4.6 mm) column. Mobile phase was methanol/water (85:15); flow rate was kept at 1 ml/min; the column temperature was 28 °C. Drug and excipients were validated to have no interference with each other.

2.5. Visualization by transmission electron microscopy (TEM)

The microstructures of HDL, TA-NLC-apo and TA-NLC were examined by TEM (H-7650, Hitachi, Japan) with negative stain method. Samples were diluted appropriately with aqueous phase before preparation for TEM. A drop of the each sample was applied to a copper grid coated with carbon film and air-dried; 2% (w/v) phosphotungstic acid (PTA) solution was then dropped onto the grids. After being negative stained and air-dried under room temperature, the samples were accomplished for the TEM investigation.

2.6. Measurement of particle size and zeta potential

Size and zeta potential of native HDL, TA-NLC and TA-NLC-apo were measured by dynamic light scattering (DLS) with a Zetasizer 3000HSA (Malvern, U.K.). Samples were diluted appropriately with aqueous phase for the measurements.

2.7. Determination of entrapment efficiency (EE) and drug loading for TA-NLC

A novel two-step method was attempted to determine EE for TA-NLC due to its tiny particle size.

Firstly, a free drug suspension (TA-SNS) was prepared without any excipients. A preparation procedure which was the same with that of TA-NLC was executed with same amount of drug. Specifically, TA was dissolved in mixture of acetone (8 ml) and absolute ethanol (2 ml) to form an organic phase maintained at 60 ± 2 °C. Then the organic phase was injected slowly into an aqueous phase of the same temperature, which contains 0.1 M KC1, 1 mM EDTA and 0.01 M Tris–HCl, pH 8.0 in double distilled water (30 ml). Then a suspension was obtained under constant magnetic agitation. After ultrasonication for 200 s using Ultrahomogenizer, the dispersion was transferred to a rotary evaporator to remove organic solvent at 65 °C under reduced pressure. The key procedure was that the final volume of TA-SNS must be equal to that of TA-NLC prepared before. Then the prepared TA-SNS was filtered through 0.22 μm filters after cooling down to room temperature.

Secondly, concentrations of TA in 0.5 ml of TA-SNS and in 0.5 ml of TA-NLC were assayed by HPLC, respectively, after dilution with absolute ethanol. EE was calculated with the following formula:

$$\text{EE } (\%) = \frac{C_0 - C}{C_0} \times 100\% \quad (2)$$

where EE is entrapment efficiency, C is the drug concentration in TA-SNS, and C_0 is the total drug concentration in TA-NLC.

Methodology of two-step method was evaluated by measuring its recovery and precisions which showed good accuracy and reproducibility (specific data will be reported in other paper). In addition, a comparison with EE obtained using dextran-gel column chromatography method for large nanoparticles showed that there were no statistic differences ($p > 0.05$) between results of the two methods.

2.8. Characterization by differential scanning calorimetry (DSC)

DSC analysis was performed using DSC 204 (NETZSCH, German). A scan rate of 10 °C min^{-1} was employed in the temperature range of 25–300 °C. Standard aluminum sample pans (10 Al) were used. An empty pan was used as reference. Preparation of samples for thermal analysis:

(A) Physical mixtures (PM). TA, cholesteryl oleate, and glycerol trioleate. The ratio of TA to matrix was similar to that of weight ratio in TA-NLC formulation.
(B) Lyophilized samples. TA-NLC and TA solid lipid nanoparticles (TA-SLN, prepared with all excipients except liquid lipid glycerol trioleate) were frozen at −70 °C for 8 h. Then the samples were freeze-dried at −52 °C and a pressure of 7.5 mmHg during 40 h. The TA-NLC and TA-SLN powder was collected and stored at 4 °C.

2.9. Electrophoretic analysis of apolipoproteins absorption on TA-NLC

2.9.1. Agarose gel electrophoresis

The electrophoretic mobilities of TA-NLC-apo, HDL and NLC were determined by electrophoresis on preformed 1% agarose gel containing barbital buffer, ionic strength = 0.05, pH 8.6. Each sample (20 μl) was directly applied to gel wells and allowed to penetrate into the gel for 5 min before the electric field was applied. A Bio-Rad model 702 power supply was used to provide a voltage of 90 ± 2 V across a gel distance of 5.5 cm. Electrophoresis was continued for 40 min at 25 ± 2 °C in barbital buffer, ionic strength = 0.075, pH 8.6. After electrophoresis, gel was stained by dripping precipitation reagent phosphotungstic acid/$MgCl_2$ (per liter, 40 g phosphotungstic acid, 0.5 mol magnesium chloride, 0.16 mol sodium hydroxide) on it for about 5 min until the background adjacent to apolipoprotein bands was clear and the stain intensity of the bands was uniform. Then the gel was photographed with gel image system (GelDoc2000, Bio-Rad, USA).

2.9.2. Sodium dodecyl sulfate polyacrylamide gel electrophoresis (SDS-PAGE)

To identify subtypes of the bound proteins on TA-NLC-apo and HDL (both has two concentrations: 2.0 mg/ml and 0.2 mg/ml) were mixed at a 4:1 (v/v) ratio with the sample buffer, respectively, then the samples were heated in boiling water for 4 min. SDS-PAGE was performed by using the Mini Protein II electrophoretic apparatus (Bio-Rad Laboratories Inc., Richmond, CA, USA) on a polyacrylamide gel consisting of 10% separating gel and a 5% stacking gel at a constant current of 15 mA/gel for about 1 h. After electrophoresis, the gel was stained with Coomassie blue R-250 (0.05%, w/v) in methanol:acetic acid:water solution (5:1:4, by volume) and destained in methanol:acetic acid:water solution without dye (1:1:8, by volume).

2.10. In vitro cell viability/cytotoxicity studies

Mouse macrophage cell line RAW 264.7 was employed to study the phagocytic uptake of TA-NLC and TA-NLC-apo. Before the study of cellular uptake, cytotoxicity was assessed by MTT assay.

Cells were routinely cultured in Dulbecco's modified eagle medium (DMEM) supplemented with 10% fetal bovine serum at 37 °C and 5% CO_2 for 3 days to attach. Prior to experiments, the medium was changed every day and the cell viability was determined to be approximately 95% by observation under microscope (COIC-XDS-1, China). Before cell viability experiments, TA-NLC was pre-incubated and mixed with same volume of native HDL for 4 h to obtain incubated TA-NLC.

Cells were plated at a density of 1×10^4 cells/well in a 96-well plate at 37 °C in 5% CO_2 atmosphere. After 24 h of culture, the medium in the wells was replaced with the fresh medium containing TA-NLC or incubated TA-NLC in varying concentrations (30, 60, 90, 120, and 150 μg/ml). After 3 h, 20 μl of MTT 3-(4,5-dimethylthiazol-2-yl)-2,5-diphenyltetrazolium bromide dye solution (5 mg/ml in phosphate buffer pH 7.4, MTT Sigma, Dorset, U.K.) was added to each well. After 4 h of incubation at 37 °C and 5% CO_2 for exponentially growing cells and 15 min for steady-state confluent cells, the medium was removed and formazan crystals were solubilized with 200 μl of DMSO and the solution was vigorously mixed to dissolve the reacted dye. The absorbance of each well was read on a microplate reader (BIO-RAD MODEL 680, USA) at 492 nm. The relative cell viability (%) related to control wells containing cell culture medium without nanoparticles was calculated by

$$\frac{[A]_{\text{test}}}{[A]_{\text{control}}} \times 100\%$$

2.11. Phagocytosis assay

Cells were treated with either 0.6 ml of incubated TA-NLC (30 μg/ml calculated by TA) or 0.6 ml of TA-NLC (ditto for concentration). After incubation periods of 1, 2 and 3 h, macrophages

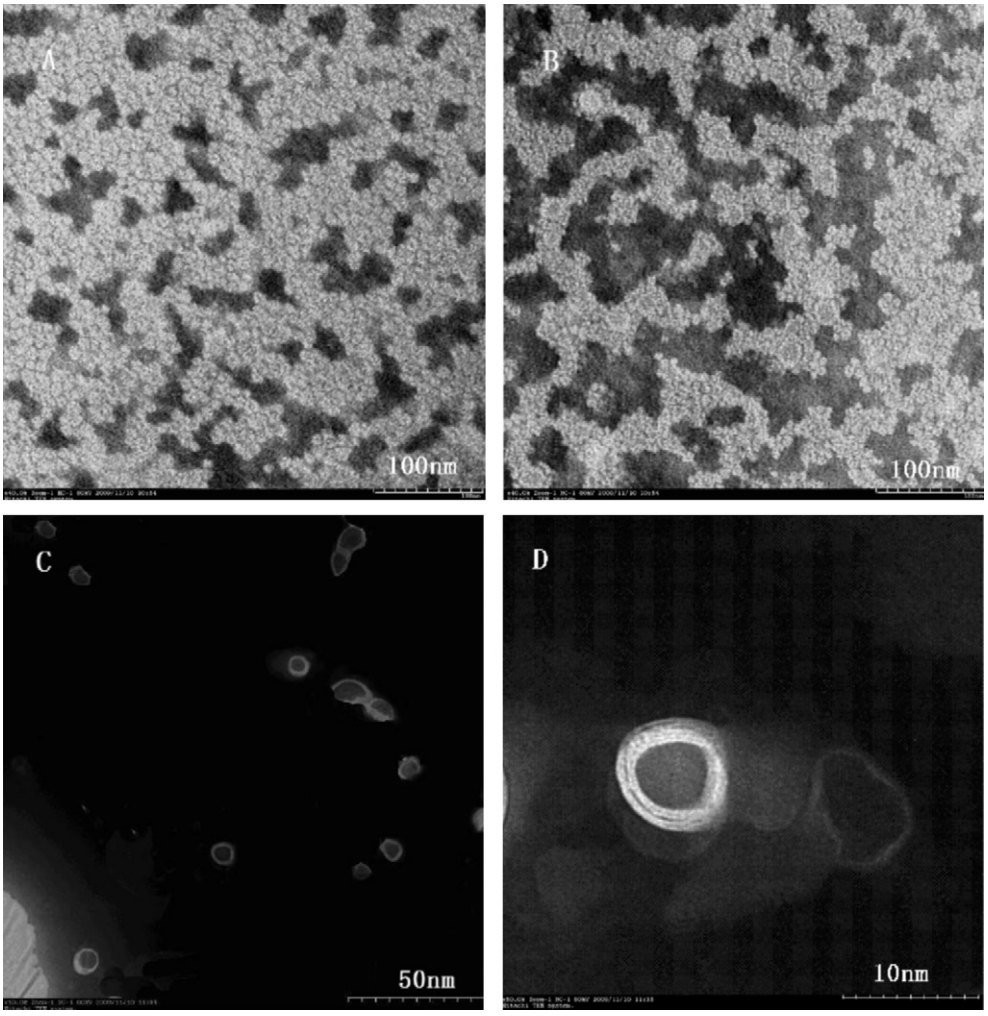

Fig. 1. Microphotographs of native HDL (A), TA-NLC-apo (B) and TA-NLC (C and D) by transmission electron microscope.

were washed and rinsed three times with Dulbecco's phosphate buffered saline (D-PBS) medium to remove the excess and non-phagocytozed nanoparticles. Then the washed macrophages were subject to five cycles of freezing and thawing to split. Nanoparticles were dissolved by adding 100 μl of methanol in each well. The amount of phagocytozed nanoparticles was determined after centrifugation by dosing HPLC Tanshinone IIA contained in macrophages. The experiments were performed in triplicate.

At last, a parallel protocol was done with TA-SNS (prepared as described above) to evaluate the phagocytosis of probable free drug present in TA-NLC. Three wells were added with 0.6 ml of aqueous phase as control.

2.12. Statistical analysis

Data reported were arithmetic mean values ± standard deviation ($\bar{x} \pm SD$). Statistically significant differences were determined using two-tailed Student's *t*-test with $p < 0.05$ or $p < 0.01$ as a level of significance.

3. Results and discussion

3.1. Visualization by transmission electron microscopy

We examined HDL, TA-NLC-apo and TA-NLC by using negative staining transmission electron microscopy and found that although some of HDL (Fig. 1A) were discoidal particles, most of them were typical spheres. In Fig. 1B, TA-NLC-apo presented heterogeneous spherical shapes. It was shown that apolipoproteins has incorporated into the lipidic corona, forming HDL-like particles. TA-NLC (Fig. 1C) were demonstrated spherical or oval particles with drug incorporated in lipid core forming a shell-core structure, which may not interfere with the external receptor-mediated recognition of apolipoproteins. The peripheral fingerprint microstructures of TA-NLC could be clearly visualized under higher-power magnification (Fig. 1D).

3.2. Characterization of TA-NLC and TA-NLC-apo

The density range of TA-NLC was 0.907–1.018 g/ml, which was lower than that of native HDL due to the lack of apolipoproteins. After centrifugation, TA-NLC all floated above the background solution (1.063 g/ml) (Fig. 2C). Native HDL isolated from blood was tint yellow (Fig. 2A) and existed at the bottom of tube against the background solution (picture not shown). After incubation with TA-NLC for 4 h, the volume of TA-NLC layer floating on the top decreased

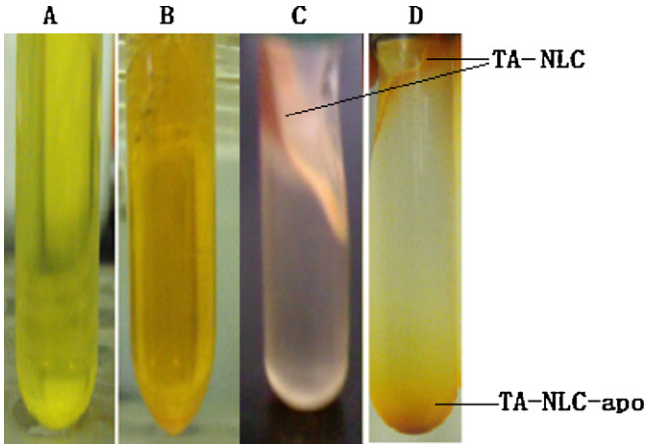

Fig. 2. Pictures of native HDL (A), TA-NLC-apo (B), TA-NLC after centrifugation (C) and TA-NLC-apo after centrifugation (D).

Table 1
Average diameter, zeta potential values (mean ± SD, $n = 3$) of HDL, TA-NLC and TA-NLC-apo.

Samples	Size (nm)	Zeta potential (mV)	PI
TA-NLC	8.0 ± 1.2[a]	−29.0 ± 0.0[b]	0.208 ± 0.093
TA-NLC-apo	8.5 ± 1.1[a]	−18.8 ± 0.0[b]	0.137 ± 0.113
HDL	8.1 ± 1.4[a]	−12.4 ± 0.1[b]	0.491 ± 0.102

PI = polydispersity index.
[a] No significant difference ($p > 0.05$).
[b] Significant difference ($p < 0.05$).

and the bottom layer has turned orange which coincided with the color of TA-NLC (Fig. 2B and D). This led to assumptions that TA-NLC has bound to apolipoproteins or complete lipoprotein particles.

Seen from Table 1, it can be observed that TA-NLC-apo, TA-NLC and native HDL were in the same size range. There were no statistic differences between them, which ruled out one of aforementioned assumptions that TA-NLC had bound to complete lipoprotein particles. The charge of native HDL was negative in pH 8.0 buffer solution which was above the isoelectric point of apolipoproteins. The surface negative charge observed in TA-NLC-apo was less than TA-NLC and more than native HDL. It was inferred that TA-NLC-apo may form a complex with a structure of TA-NLC core surrounded by apolipoproteins. As for TA-NLC and native HDL, their different charge may result from discrepancy in apolipoproteins and particle size.

The TA-NLC maintained excellent stability without exhibiting any aggregation, precipitation, and phase separation at 4 °C for 6 weeks of storage. It displayed better stability than TA-SLN reported before (Zhang et al., 2008), which may be attributed to the fact that admixture of liquid lipids with solid lipids lead to a less ordered inner structure of NLC which has the minimum incidence of drug expulsion during storage (Jenning et al., 2000).

3.3. Entrapment efficiency and drug loading of TA-NLC

During preliminary studies, we have discovered that dextran-gel column chromatography method could not separate TA-NLC from free drug completely. The probable reason was that their size was in close proximity with each other. In this experiment, a two-step method was employed with a principle that the concentration of free drug either in the TA-NLC or TA-SNS was the same. This was because free drug evenly dispersed in two formulations was at a saturated state under parallel operation condition after filteration. Therefore, the concentration of unencapsulated drug in TA-NLC can be obtained by determining the drug concentration of TA-SNS.

The prepared free drug suspension looked even and transparent after filtering out large drug granules. The size distribution of free drug suspension as measured by DLS showed one narrow peak indicating that the particulate population was relatively homogenous in size. The EE for TA-NLC was 97.84 ± 1.2%, and the drug loading was 6.17 ± 0.3%, which was 1.5 times higher than TA-SLN reported before (Zhang et al., 2008) due to the wide diversity of the drug solubility in the vehicle components and low crystallinity of lipid with high compatibility (Souto et al., 2004). Thus, the drug molecules can be accommodated in between lipid layers and/or fatty acid chains (Müller et al., 2002b).

3.4. Characterization by differential scanning calorimetry (DSC)

DSC has been used to characterize the melting and crystallization behavior of crystalline material like lipid nanoparticles (Hu et al., 2006; Han et al., 2008). In the case of NLC, DSC characterization can illuminate its structure through the mixing behavior of solid lipids with liquid lipids.

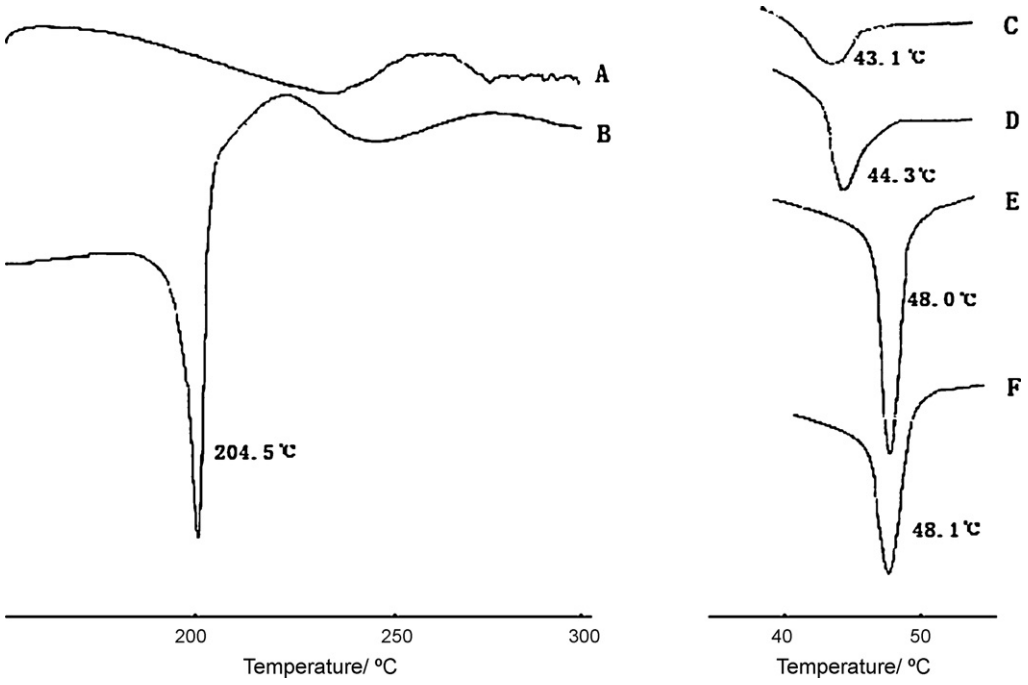

Fig. 3. Overlaid DSC thermograms of lyophilized TA-NLC (A and C), physical mixtures (B and F), lyophilized TA-SLN (D) and bulk cholesteryl oleate (E).

In Fig. 3 were reported the thermograms obtained from bulk material (cholesteryl oleate), TA, PM, lyophilized samples (TA-NLC and TA-SLN).

The thermograms of the lyophilized TA-NLC (A) did not show the melting peak of the TA around 204.5 °C. This indicated that TA in the TA-NLC was not in crystalline state but in amorphous state. Similar results were reported by Venkateswarlu and Manjunath (2004) stating that method of preparation (ultrasonication) could not allow the drug to crystallize. However, the presence of TA crystalline state was confirmed by the melting peak of TA in the PM (B). The noticeable depression of the melting point of cholesteryl oleate in TA-NLC (C) or TA-SLN (D) with respect to the bulk cholesteryl oleate (E) appeared consistent with "Kelvin effect". That is due to small particle size and the high specific surface area (Venkateswarlu and Manjunath, 2004; Hu et al., 2005).

Crystallinity (C%), which is defined as the percentage of the lipid matrix that has recrystallized, was a useful parameter to investigate the physical state of lipid matrix in TA-NLC. The C% can be calculated according to the following equation (Freitas and Müller, 1999):

$$C\% = \frac{\text{enthalpy}_{\text{freeze-dried NLC or SLN}}}{\text{enthalpy}_{\text{bulk}}} \times 100\%$$

The enthalpy and crystallinity of each sample were listed in Table 2. The results showed that, compared with bulk materials, crystallinity of samples in nanometer system was lower than initial lipid and the lowest one was TA-NLC. This result was an indication that glycerol trioleate was the main reason for perfect crystal order disturbance (lattice defects) and defect increasing in NLC (Jenning et al., 2000). The less ordered modification could allow more space to accommodate drug molecules, thus leading to total drug loading capacity improvement.

Table 2
Melting peaks, enthalpies and crystallinity of bulk cholesteryl oleate, PM, lyophilized TA-SLN and TA-NLC.

Sample	Melting points (°C)	Enthalpy (J/g)	Crystallinity (%)
Bulk	48.0	111.2	100
PM	48.1	110.6	99.5
TA-SLN	44.3	71.7	64.5
TA-NLC	43.1	37.6	33.8

3.5. Apolipoprotein-binding properties of TA-NLC

The electrophoretic migration of TA-NLC-apo, native HDL and TA-NLC was shown in Fig. 4.

Since phosphotungstic acid/$MgCl_2$ can be used for complete precipitation of apolipoprotein-B containing lipoproteins in hypertriglyceridemic sera with only marginal co-precipitation of HDL (Assmann et al., 1983), it can be employed as stain agent for proteins in this experiment, which possessed simple and convenient procedures and favorable staining effect. As shown in Fig. 4(1), either native HDL or TA-NLC-apo presented a white band under white light which may contain one population of particles based on charge, while no stain was observed for TA-NLC. Moreover, TA-NLC-apo migrated faster than native HDL (Lou et al., 2005), which might demonstrate changed composition of native HDL after incubation with TA-NLC. In addition, white bands gave evidence of apolipoproteins contained in HDL and TA-NLC-apo, but not in TA-NLC. More negative charge in TA-NLC-apo than native HDL, as indicated by their zeta potentials, might result in faster mobility of TA-NLC-apo to anode than native HDL.

Fig. 4(2) shows electrophoretic pattern with a same agarose gel observed in ultraviolet light. TA-NLC and TA-NLC-apo presented white bands due to Tanshinone II A fluorescence under ultraviolet light illumination, and no stain was observed for native HDL accordingly, therefore we inferred that TA-NLC-apo was a complex of TA-NLC and apolipoproteins, as indicated earlier by their changed color. Moreover, drug was shown to migrate in forms of drug loading particles rather than free drug due to the high molecular weight of band C in Fig. 4(2) as well as the consistent positions of band A between Fig. 4(1) and (2).

Fig. 5 shows the SDS-PAGE patterns of apolipoproteins on native HDL and TA-NLC-apo with different concentrations.

As shown in Fig. 5(1), bands of apoA-I with molecular weight of 28 kDa were thickest for both A and B, which indicated that apoA-I was the predominant apolipoprotein that bound to TA-NLC,

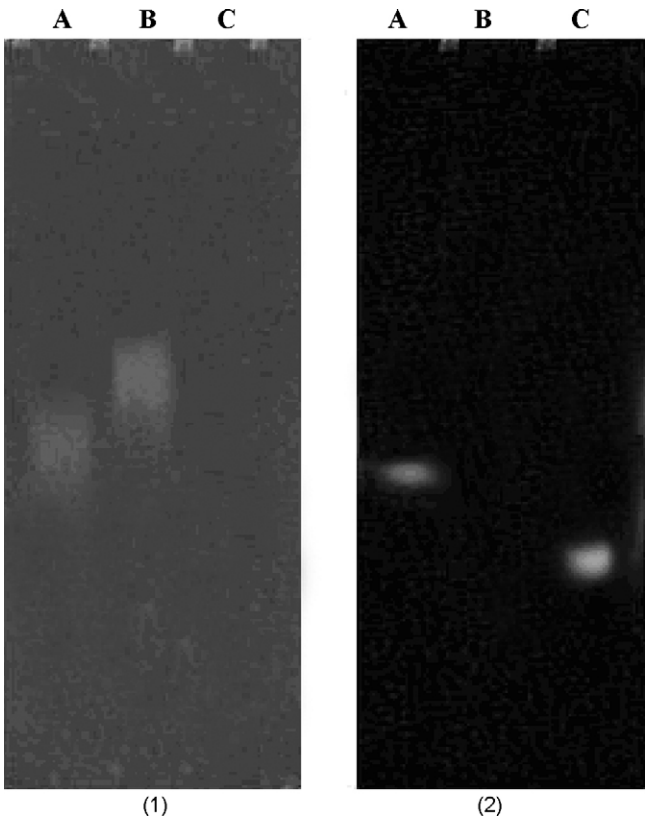

Fig. 4. Agarose gel electrophoretic patterns observed in white light (1) and ultraviolet light (2). (A) TA-NLC-apo; (B) native HDL; (C) TA-NLC.

although residues of other apolipoproteins with molecular weight lower than 29 kDa could also be seen. However, compared to native HDL (B), the content of apolipoproteins on TA-NLC-apo (A) was much less.

Fig. 5(2) shows thicker apoA-I bands as well as bands of apolipoproteins with higher molecular weight. It was notable that A and B possessed same staining bands position except for the band of apoE with molecular weight of 34 kDa. Specifically, the band of apoE was absent for TA-NLC-apo, whereas the content of apoE in native HDL was considerable.

Two important conclusions may be drawn from aforementioned phenomena: (1) Since all bands of apolipoproteins on native HDL were not presented proportionally on SDS-PAGE pattern for TA-NLC-apo, it was again confirmed that TA-NLC-apo might be complex of TA-NLC and apolipoproteins rather than that of TA-NLC and native HDL. (2) TA-NLC could bind to apoA-I specifically, which related to its particle size and density (Pittman et al., 1987; Galeano et al., 1994; Göppert and Müller, 2005; Hellstrand et al., 2009) and shared a similar mechanism with lipid emulsion (resembling low density lipoprotein) binding to apoE specifically (Maranhao et al., 1994; Ginsburg et al., 1982). It was reported that a Pro residue, which was necessary to define the structural and functional properties of apoA-I, associated mostly with small lipoproteins (HDL). In contrast, the apoE lipid-binding domain associates with larger lipoproteins (Segrest et al., 1994).

3.6. Cytotoxicity studies

The results indicated that incubated TA-NLC revealed little cytotoxic effects to cells and they remained 95% in viable relative to control. However, TA-NLC showed significant loss in viability of about 12–24%. One possible explanation for this decrease in cell viability may be that TA-NLC are taken up by the cells as a result of

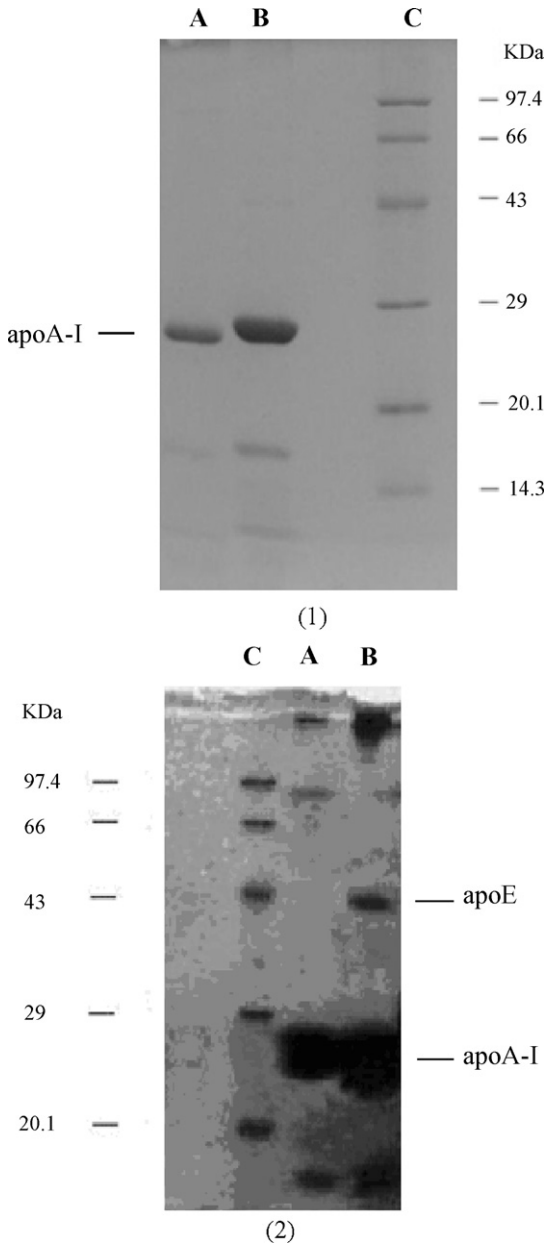

Fig. 5. The SDS-PAGE patterns of TA-NLC-apo and native HDL with different concentrations of 0.2 mg/ml (1) and 2.0 mg/ml (2). (A) TA-NLC-apo; (B) native HDL; (C) molecular weight standards.

endocytosis or are promoting apoptosis (programmed cell death). The low toxicity of incubated TA-NLC may be attributed to the apolipoproteins crowned on TA-NLC after incubation with native HDL, which are biocompatible, nonimmunogenic, and nonantigenic. It was reported that the surface characteristics of particulate determined how the nanoparticles will adsorb to the cell surface and more particularly determined the cell behavior on contact (Gupda and Wells, 2004).

3.7. Uptake of nanoparticles by murine macrophages

Mouse macrophage cell line RAW264.7 was employed to evaluate the helping effect of apolipoproteins bound to TA-NLC to escape phagocytosis.

As proved in early experiments, TA-NLC could bind to apolipoproteins after incubation with native HDL. So TA-NLC-apo can be used to represent the predominant component of incubated

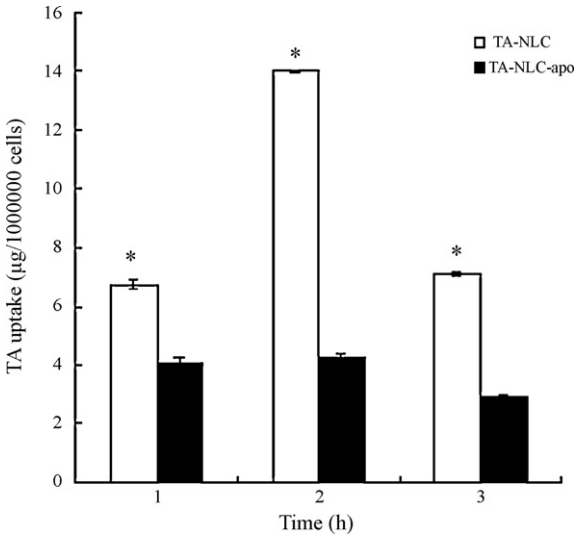

Fig. 6. Uptake of TA-NLC and TA-NLC-apo by murine macrophages after different incubation periods ($n = 3$). Results are expressed as the amount of TA phagocytozed with respect to 1,000,000 cells. $^{*}p < 0.01$, statistical significances with TA-NLC vs. TA-NLC-apo (error bars represent the standard deviation).

TA-NLC. The uptake of free TA present in TA-NLC suspensions has been determined to be 0.608 ± 0.05 μg/10^6 cell and was subtracted from assay results for sake of precision.

The results in Fig. 6 showed significant differences in phagocytosis uptake between TA-NLC and TA-NLC-apo. It was noted that the uptake of TA-NLC increased with time. However, this behavior was not so obvious for TA-NLC-apo. After incubation with native HDL, TA-NLC turned endogenous by crowning with apolipoproteins, which cannot trigger immunological responses and could escape from recognition by macrophages (Lou et al., 2005). Also, the uptake of both TA-NLC and TA-NLC-apo in 3 h was lower than that in 2 h. The likely explanation was that the phagocytosis of macrophages had a peak value between 2 h and 3 h. Macrophages phagocytozing plenty of nanoparticles floated in the DMEM after 3 h and were washed away by D-PBS (Feng et al., 2005).

Judging from the uptake data of TA-NLC-apo shown in Fig. 6, we knew that TA-NLC was not exclusively present in association with apolipoproteins after incubation, although the amount of native HDL was higher than that of TA-NLC during incubation, which revealed that per TA-NLC particle may associate with more apolipoprotein molecules (mainly apoA-I) than native HDL.

4. Conclusion

The present work concerns the development of an HDL-like NLC to serve as a model in which to study lipid–apolipoprotein interaction and develop a naturally long-circulating, health beneficial and controlled-release delivery system.

In this paper, we prepared TA-NLC with properties such as size range, shape and composition resembling the lipid portion of native HDL. Due to the spacial nanostructure of lipid mixture formed in TA-NLC, drug loading and stability were greatly improved. The *in vitro* incubation tests confirmed that TA-NLC could bind to apoA-I specifically. Macrophage studies demonstrated that TA-NLC incubated with native HDL could turn endogenous by association to apolipoproteins, which cannot trigger immunological responses and could escape from recognition by macrophages.

Therefore, HDL-mimicking NLC would provide highly desirable physicochemical characteristics as a delivery vehicle of lipophilic cardiovascular drug.

References

Ajees, A.A., Anantharamaiah, G.M., Mishra, V.K., Hussain, M.M., Murthy, H.M.K., 2006. Crystal structure of human apolipoprotein A-I: insights into its protective effect against cardiovascular diseases. Proc. Natl. Acad. Sci. U.S.A. 103, 2126–2131.

Assmann, G., Nofer, J.R., 2003. Atheroprotective effects of high-density lipoproteins. Annu. Rev. Med. 54, 321–341.

Assmann, G., Schriewer, H., Schmltz, G., hägele, E.O., 1983. Quantification of high-density-lipoprotein cholesterol by precipitation with phosphotungstic Acid/$MgCl_2$. Clin. Chem. 29, 2026–2030.

Bunjes, H., Koch, M.H.J., Westesen, K., 2003. Influence of emulsifiers on the crystallization of solid lipid nanoparticles. J. Pharm. Sci. 92, 1509–1520.

Calabresi, L., Gomaraschi, M., Rossoni, G., Franceschini, G., 2006. Synthetic high density lipoproteins for the treatment of myocardial ischemia/reperfusion injury. Pharmacol. Ther., 111.

Chu, M.Q., Gu, H.C., Liu, G.J., 2002. Study on the preparation of tanshinone proliposomes by spray drying method. Zhongguo Yao Xue Za Zhi 37, 32–35.

Cormode, D.P., Skajaa, T., Schooneveld, M.M., Koole, R., Jarzyna, P., Lobatto, M.E., Calcagno, C., Barazza, A., Gordon, R.E., Zanzonico, P., Fisher, E.A., Fayad, Z.A., Mulder, W.J.M., 2008. Nanocrystal core high-density lipoproteins: a multimodality contrast agent platform. Nano Lett. 8, 3715–3723.

Eriksson, M., Carlson, L.A., Miettinen, T.A., Angelin, B., 1999. Stimulation of fecal steroid excretion after infusion of recombinant proapolipoprotein A-I: potential reverse cholesterol transport in humans. Circulation 100, 594–598.

Feng, M., Pan, S.R., Zhang, J.X., Wang, Q.M., Wu, W.R., Li, R.M., 2005. *In vitro* phagocytic uptake of PEG-PBLG nanoparticles containing amphotericin B. J. Chin. Pharm. Univ. 36, 321–325.

Fessi, H., Puisieux, F., Devissaguet, J.P., Ammoury, N., Benita, S., 1989. Nanocapsule formation by interfacial polymer deposition following solvent displacement. Int. J. Pharm. 55, R1–R4.

Freitas, C., Müller, R.H., 1999. Correlation between long-term stability of solid lipid nanoparticles (SLN™) and crystallinity of the lipid phase. Eur. J. Pharm. Biopharm. 47, 125–131.

Frias, J.C., Ma, Y., Williams, K.J., Fayad, Z.A., Fisher, E.A., 2006. Properties of a versatile nanoparticle platform contrast agent to image and characterize atherosclerotic plaques by magnetic resonance imaging. Nano Lett. 6, 2220–2224.

Galeano, N.F., Milne, R., Marcel, Y.L., Walsh, M.T., Levy, E., Ngu'yen, T.D., Gleeson, A., Arad, Y., Witte, L., Al-Haideri, M., Rumsey, S.C., Deckelbaum, R.J., 1994. Apoprotein structure and receptor recognition of triglyceride-rich low density lipoprotein (LDL) is modified in small but not in triglyceride-rich LDL of normal size. J. Biol. Chem. 269, 511–519.

Ginsburg, G.S., Small, D.M., Atkinson, D., 1982. Microemulsions of phospholipids and cholesteryl esters: protein-free models of low density lipoprotein. J. Biol. Chem. 257, 8216–8227.

Göppert, T.M., Müller, R.H., 2005. Adsorption kinetics of plasma proteins on solid lipid nanoparticles for drug targeting. Int. J. Pharm. 302, 172–186.

Gupda, A.K., Wells, S., 2004. Surface-modified superparamagnetic nanoparticles for drug delivery: preparation, characterization, and cytotoxicity studies. IEEE Trans. Nanobiosci. 3, 66–73.

Han, F., Li, S., Yin, R., Liu, H., Xu, L., 2008. Effect of surfactants on the formation and characterization of a new type of colloidal drug delivery system: nanostructured lipid carriers. Colloids Surf. A: Physicochem. Eng. Aspects 315, 210–216.

Hao, H., Wang, G., Cui, N., Li, J., Xie, L., Ding, Z., 2007. Identification of a novel intestinal first pass metabolic pathway: NQO1 mediated quinone reduction and subsequent glucuronidation. Curr. Drug Metab. 8, 137–149.

Hellstrand, E., Lynch, I., Andersson, A., Drakenberg, T., Dahlbäck, B., Dawson, K.A., Linse, S., Cedervall, T., 2009. Complete high-density lipoproteins in nanoparticle corona. FEBS J. 276, 3372–3381.

Herbert, P.N., Bernier, D.N., Cullinane, E.M., Edelstein, L., Kantor, M.A., Thompson, P.D., 1984. High-density lipoprotein metabolism in runners and sedentary men. JAMA 252, 1034–1037.

Hu, F.Q., Jiang, S.P., Du, Y.Z., Yuan, H., Ye, Y.Q., Zeng, S., 2005. Preparation and characterization of stearic acid nanostructured lipid carriers by solvent diffusion method in an aqueous system. Colloids Surf. B: Biointerfaces 45, 167–173.

Hu, F.Q., Jiang, S.P., Du, Y.Z., Yuan, H., Ye, Y.Q., Zeng, S., 2006. Preparation and characteristics of monostearin nanostructured lipid carriers. Int. J. Pharm. 314, 83–89.

Jenning, V., Thünemann, A.F., Gohla, S.H., 2000. Characterisation of a novel solid lipid nanoparticle carrier system based on binary mixtures of liquid and solid lipids. Int. J. Pharm. 199, 167–177.

Joshi, M., Pathak, S., Sharma, S., Patravale, V., 2008. Design and in vivo pharmacodynamic evaluation of nanostructured lipid carriers for parenteral delivery of artemether: nanoject. Int. J. Pharm. 364, 119–126.

Kontush, A., Chapman, M.J., 2006. Functionally defective high-density lipoprotein: a new therapeutic target at the crossroads of dyslipidemia, inflammation, and atherosclerosis. Pharmacol. Rev. 58, 342–374.

Li, H.L., Zhang, Z.Y., Ma, L.L., Chen, X.Y., 2007a. Preparation of tanshinone microemulsion and its absorption in rat intestine in situ. Zhongguo Zhong Yao Za Zhi 32, 1024–1027.

Li, Q., Wang, Y., Feng, N., 2008. Novel polymeric nanoparticles containing tanshinone IIA for the treatment of hepatoma. J. Drug Target 16, 732.

Li, X., Li, X., Wang, L., Li, Y., Xu, Y., Xue, M., 2007b. Simultaneous determination of danshensu, ferulic acid, cryptotanshinone and tanshinone IIA in rabbit plasma by HPLC and their pharmacokinetic application in danxiongfang. J. Pharm. Biomed. Anal. 44, 1106–1112.

Liang, L., Chen, Y., Xiong, S., Zeng, Z., Sun, M., Zhang, H., 2007. The inhibitive effect produced by local perfusion of tanshinone IIA nanoparticle on neointimal hyper-

plasia of rabbit carotid artery following intimal denudation. Sheng Wu Yi Xue Gong Cheng Xue Za Zhi 24, 812–816.
Liang, Z., Mao, S.J., Yin, Z.N., Jin, H., Li, H., Chu, T., 2008. Preparation and quality evaluation of intravenous tanshinone II (A) emulsion. Zhongguo Zhong Yao Za Zhi 33, 1249–1252.
Libby, P., Bonow, R., Mann, D., Zipes, D., 2008. Braunwald's Heart Disease: A Textbook of Cardiovascular Medicine, 8th ed. Saunders Elsevier, Philadelphia, PA.
Linsel-Nitschke, P., Tall, A.R., 2005. HDL as a target in the treatment of atherosclerotic cardiovascular disease. Nat. Rev. Drug Discov. 4, 193–205.
Liu, J.P., Zhu, J.B., Du, Z.Y., Qin, B., 2005. Preparation and pharmacokinetic evaluation of tashinone II a solid lipid nanoparticles. Drug Dev. Ind. Pharm. 31, 551–556.
Lou, B., Liao, X.L., Wu, M.P., Cheng, P.F., Yin, C.Y., Fei, Z., 2005. High-density lipoprotein as a potential carrier for delivery of a lipophilic antitumoral drug into hepatoma cells. World J. Gastroenterol. 11, 954–959.
Mallory, J.B., Kushner, P.J., Protter, A.A., Cofer, C.L., Appleby, V.L., Lau, K., Schilling, J.W., Vigne, J.L., 1987. Expression and characterization of human apolipoprotein A-I in Chinese hamster ovary cells. J. Biol. Chem. 262, 4241–4247.
Maranhao, R.C., Cesar, T.B., Pedroso-Mariani, S.R., Hirata, M.H., Mesquita, C.H., 1993. Metabolic behavior in rats of a nonprotein microemulsion resembling low-density lipoprotein. Lipids 28, 691–696.
Maranhao, R.C., Garicochea, B., Silva, E.L., Dorlhiac-Llacer, P., Cadena, S.M.S., Coelho, I.J.C., Meneghetti, J.C., Fileggi, F.J.C., Chamone, D.A.F., 1994. Plasma kinetics and biodistribution of a lipid emulsion resembling low-density lipoprotein in patients with acute leukemia. Cancer Res. 54, 4660–4666.
McConathya, W.J., Nair, M.P., Paranjapea, S., Mooberry, L., Lacko, A.G., 2008. Evaluation of synthetic/reconstituted high-density lipoproteins as delivery vehicles for paclitaxel. Anticancer Drugs 19, 183–188.
Müller, R.H., Radtke, M., Wissing, S.A., 2002a. Nanostructured lipid matrices for improved microencapsulation of drugs. Int. J. Pharm. 242, 121–128.
Müller, R.H., Radtke, M., Wissing, S.A., 2002b. Solid lipid nanoparticles (SLN) and nanostructured lipid carriers (NLC) in cosmetic and dermatological preparations. Adv. Drug Deliv. Rev. 54, 131–155.
Oda, M.N., Hargreaves, P.L., Beckstead, J.A., Redmond, K.A., Antwerpen, R., Ryan1, R.O., 2006. Reconstituted high-density lipoprotein enriched with the polyene antibiotic amphotericin B. J. Lipid Res. 47, 260–267.
Pittman, R.C., Glass, C.K., Atkinson, D., Small, D.M., 1987. Synthetic high density lipoprotein particles. J. Biol. Chem. 262, 2435–2442.
Pyle, L.E., Sawyer, W.H., Fujiwara, Y., Mitchell, A., Fidge, N.H., 1996. Structural and functional properties of full-length and truncated human proapolipoprotein AI expressed in *Escherichia coli*. Biochemistry 35, 12046–12052.
Radding, C.M., Steinberg, D., 1960. Studies on the synthesis and secretion of serum lipoproteins by rat liver slices. J. Clin. Invest. 10, 1560–1569.
Rensen, P.C.N., Vrueh, R.L.A., Kuiper, J., Bijsterbosch, M.K., Biessen, E.A.L., Berkel, T.J.C., 2001. Recombinant lipoproteins: lipoprotein-like lipid particles for drug targeting. Adv. Drug Deliv. Rev. 47, 251–276.
Schöler, N., Hahn, H., Müller, R.H., Liesenfeld, O., 2002. Effect of lipid matrix and size of solid lipid nanoparticles (SLN) on the viability and cytokine production of macrophages. Int. J. Pharm. 231, 167–176.
Segrest, J.P., Garber, D.W., Brouillette, C.G., Harvey, S.C., Anantharamaiah, G.M., 1994. The amphipathic a helix: a multifunctional structural motif in plasma apolipoproteins. Adv. Protein Chem. 45, 303–369.
Silva, R., Huang, R., Morris, J., Fang, J., Gracheva, E.O., Ren, G., Kontush, A., Jerome, W.G., Rye, K.A., Davidson, W.S., 2008. Structure of apolipoprotein A-I in spherical high density lipoproteins of different sizes. Proc. Natl. Acad. Sci. U.S.A. 105, 12176–12181.
Souto, E.B., Wissing, S.A., Barbosa, C.M., Müller, R.H., 2004. Development of a controlled release formulation based on SLN and NLC for topical clotrimazole delivery. Int. J. Pharm. 278, 71–77.
Thaxton, C.S., Daniel, W.L., Giljohann, D.A., Thomas, A.D., Mirkin, C.A., 2009. Templated spherical high density lipoprotein nanoparticles. J. Am. Chem. Soc. 131, 1384–1385.
Thomas, M.J., Bhat, S., Sorci-Thomas, M.G., 2008. Three-dimensional models of HDL apoA-I: implications for its assembly and function. J. Lipid Res. 49, 1875–1883.
Vance, D.E., Vance, J.E., 2002. Biochemistry of Lipids, Lipoproteins and Membranes, 4th ed. Elsevier Science, Amsterdam.
Venkateswarlu, V., Manjunath, K., 2004. Preparation, characterization and in vitro release kinetics of clozapine solid lipid nanoparticles. J. Control. Release 95, 627–638.
Zhang, W.L., Liu, J.P., Li, S.C., Chen, M.Y., Liu, H., 2008. Preparation and evaluation of stealth tashinone IIA-loaded solid lipid nanoparticles: influence of Poloxamer 188 coating on phagocytic uptake. J. Microencapsul. 25, 203–209.
Zhao, B.L., Jiang, W., Zhao, Y., Hou, J.W., Xin, W.J., 1996. Scavenging effects of Savia miltiorrhiza on free radical and its protection for myocardial mitochondrial membranes from ischemia-reperfusion injury. Biochem. Mol. Biol. Int. 38, 1171–1182.